Chapter 2. Theoretical Background

2.1 Introduction

Ferrites are the ferrimagnetic oxide which are semiconductors in nature, opened another entryway in material science. The necessity of ferrites with high resistivity led to synthesize different type of ferrites. The rising interest of low loss ferrites provoked in detail investigations on the different features of its conductivity and the effect of the different dopants on the structure, electrical and thermoelectric properties, hall mobility etc. The structural, magnetic and electrical properties of ferrites hinge on numerous factors such as preparation technique, synthesis parameters, site preference and cation distribution etc. [145-147].

In this chapter different theory, mathematical formulae for structural, dielectric, electrical and magnetic behaviors of ferrite and various synthesis procedures are briefly discussed. These theoretical models and formulae help in different ways for analysis, evaluation, conclusion and discussion of the outcomes obtained. Hence different theoretical models and synthesis techniques have been illustrated which endorse to understand the properties of ferrites.

2.2 Synthesis techniques

A small amount of non-magnetic substitution can drastically change the properties of magnetic materials. So these are very conscious to its preparation procedure, processing parameters and impurity levels. In this manner the choice of synthesis technique for the ferrites and its composites is exceptionally critical. This guarantee to get profoundly pure single phasic materials. There are bunches of approach accessible for synthesizing ferrite materials. Here some preparation methods are briefly discussed.

2.2.1 Solid state reaction method

The most versatile technique of synthesizing different metal oxides and other solid materials is solid state reaction technique or ceramic technique which include grinding of metal oxides, metal carbonates, metal oxalates or other compounds of relevant metals and heating the mixed powder at high temperature. Several oxides, sulphides, phosphides etc. have been prepared by this method. This method is exceptionally straightforward and advantageous than the other methods. The main drawback of this technique is that the last materials may have some extra phases. Vital strides in this route are calcinations and sintering. Time and temperature for calcination and sintering varies for different systems. In this method pure metal oxides are taken and mixed thoroughly and uniformly. This mixture is sintered for long time at particular temperature to expedite chemical reaction and the formation of desire product. Calcination temperature of the samples may about 1000^{o}C and the final sintering temperature of the ferrite sample is about 1200^{o}C depending on the contents of the sample.

2.2.2 Sol-gel auto combustion technique

Sol-gel auto combustion method or the self-propagating high temperature synthesis is another very common technique for preparing is of a range of solid materials [148]. In this technique there is high exothermic reaction between the starting materials. As a result, a combustion flame has been produced and we will get the expected product. The combustion method has been accomplished in air or oxygen to develop the complex metal

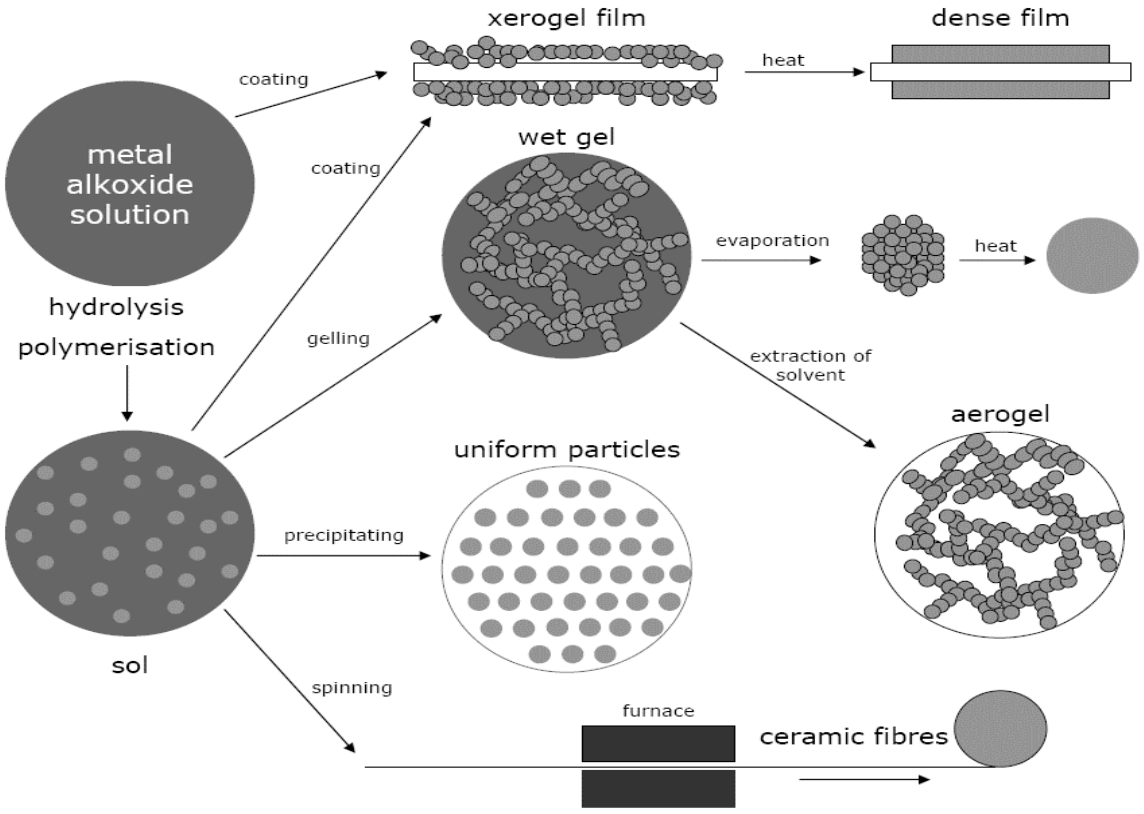

Fig. 2.1. Schematic representation of different steps involve in Sol-Gel technique.

oxides. As of late, an expansive quantities of oxides have been produced by utilizing nitrate mixture with a fuel, for example, glycerin, urea and tetra formal hydrazine. Fine oxide powders can be acquired by heating powder using the combustion. In some rare cases, the

desired material can obtained directly. Materials like metal oxides, borides, carbides, and other compounds of metal have been synthesized by using this method. To make combustion, the mixture of raw materials with high chemical energy are highly dispersed. Sometimes an oxidizer or fuel have been to ensure the combustion take place. The mixture of starting materials is mostly kept in a particular gas medium which help to start exothermic reaction. Depending on the reaction the combustion temperature may vary from 150 K to 300 K. since the final product can be found out soon after combustion, hence, the reaction time is too short. This method have also been used to prepare superconducting Cuprites. The steps involve in the Sol-Gel method is illustrated in Fig. 2.1.

2.2.3 Hydrothermal technique

This technique involves different methods in which high-temperature aqueous solutions are used at high vapor pressures results in crystallization of substances. The term "hydrothermal" have the origin from geology. Since the beginning of 20th century several mineralogists and geochemists have investigated hydrothermal phase equilibrium. George W. Morey from Carnegie Institution and Percy W. Bridgman from Harvard University have worked to find the necessary condition for the reactive medium in the range of pressure and temperature where most of the hydrothermal method is organized. The steps involve in the hydrothermal technique is shown in Fig. 2.2.

Hydrothermal technique is defined as a technique to prepare single crystals materials which relies upon the hot water solubility of minerals under high vapor pressure. The crystal growth is done in a steel pressure container, called autoclave. Between the two

ends of the container there is a temperature gradient. The contents are dissolves at the hotter end, whereas at the cooler end, it is deposited on crystal seed.

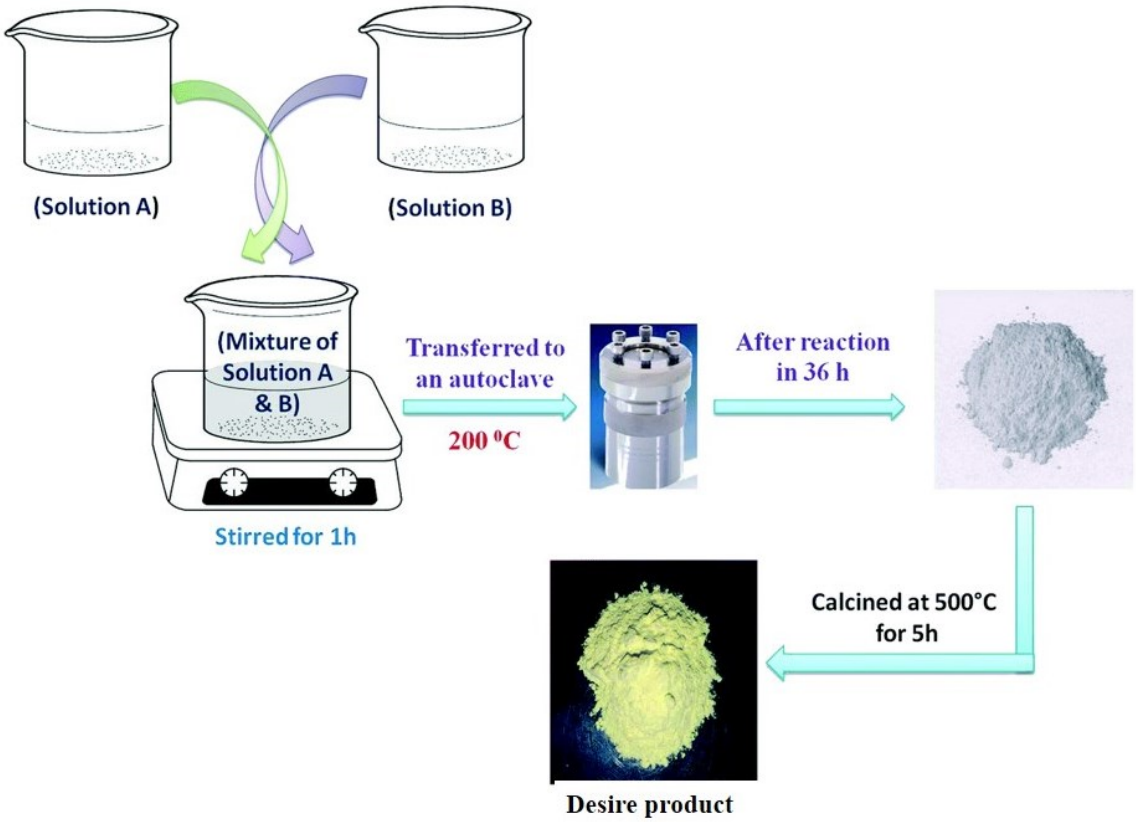

Fig. 2.2. Schematic representation of different steps involve in hydrothermal technique.

The primary advantages of the hydrothermal process compare to other methods is the ability to produce the desire materials which are unstable at their melting point. Likewise, materials having high vapor pressure near melting points can likewise be made by utilizing the hydrothermal technique. The technique is also convenient to create large types of material with better control of their composition. The main disadvantages of the process is that it requires expensive autoclaves and the crystal growth is impossible to observe.

2.2.4 Citrate precursor technique

Citrate precursor technique involve individual cations in the stoichiometric proportion are responded with the poly functional organic acid or citric acid under governed pH to acquire a precursor at an atomic level bending of the constituent components in the appropriate stoichiometric proportion is accomplished at the time of the reaction in the solution state to produce the citrate complex.

This precursor on appropriate thermal decomposition at a specific temperatures demonstrated by thermal analysis data loses all the organic moiety to offer ascent to the desire ternary oxide. It's noted that the diffusion governed solid state reaction among constituent compounds included in ceramic route and co-precipitation route is absent in the precursor technique. The last step is the decomposition process and it relies upon the decomposition temperature of the precursor. The citrate precursors decompose at temperature less than 700^{o}C and hence it has been conceivable to synthsize barium hexaferrite and series of rare earth garnet at at these moderately low temperatures.

In this way on a basic level, on the off chance that one can get precursor complexes utilizing organic completing materials not citrates, then it will decompose at lower temperatures compare to citrate. The preparation temperature may be possible for further reduction. Reducing the preparation temperature will be extremely vital for synthesis of nano particles of the hexaferrite system.

2.2.5 Co-precipitation technique

Chemical co-precipitation technique (CPT) refer to the precipitation of substances which generally soluble under different conditions imposed on it. In medicinal science, co-precipitation involves the precipitation of a loose antigen with antigen-antibody complex. In chemistry, co-precipitation is a crucial term in chemical analysis. Co-precipitation is used to estimate the mass of precipitated analyte in gravimetric analysis to determine the purity and concentration. But there is a problem with co-precipitation due to impurity precipitation, results in excess in mass. This could be mollify by digestion or re-dissolve the sample and precipitate it again.

Furthermore, in radiochemistry to analyze of trace elements, co-precipitation is often used to separate an element. Precipitation of trace element is difficult because the trace element may too dilute (sometimes less than parts per trillion). Hence, it is co-precipitated with a carrier substance with similar crystalline structure which can assimilate the element. Co-precipitation is used to separate francium from other radioactive elements by co-precipitating caesium salts such as caesium perchlorate. Otto Hahn promoted the use of co precipitation in radiochemistry. Co-precipitation technique includes three mechanisms such as, inclusion, occlusion and adsorption. In inclusion the impurity incorporate in the lattice site of the carrier crystal which create crystallographic defect. This will occur when the charge and ionic radius of impurity are of the same order to those of carrier. When the bound impurity get substantially captured in the crystal, the occlusion will happen. Besides its applications in radiochemistry and chemical analysis, the co-precipitation technique is also used in many environmental related issues such as water

resources, wastewater treatment technology, acid mine drainage, metal contaminant transport at industrial and defense sites, radionuclide migration in fouled waste repositories and metal concentrations in aquatic systems ". Co-precipitation is primarily utilized to synthesize magnetic nano-material.

2.2.6 Spray pyrolysis method

Spray pyrolysis method is also a common method to prepared ferrite thin films by using a citrate complex precursor. This synthesis technique basically resides two steps. The first one is to prepared the citrate complex precursor and the second one is to spray deposition of the films by the solution of precursor. Firstly the aqueous solutions of nitrates of Ba and Fe in stoichiometric ratio were made. This solution and the citric acid are taken in 1:1 molar ratio reacted under proper pH conditions. The reaction occurred in a light alkaline media. For that ammonia solution was added drop by drop to the reactant with constant stirring as far as the expected pH is gained. Then the solution is refluxed for 6 h with proper pH condition to complete the reaction form citrate complex precursor. To obtain the homogeneous single-phase films the vital step is the preparation of the citrate complex precursor. Therefore when the right complex is obtained, at particular low temperature the ternary oxide phase can be formed by thermal decomposition of the complex. Hence, cleaned quartz plates is taken and the diluted precursor solution is sprayed at 350-400^{o}C and dried by using dry nitrogen as carrier gas. Therefore a homogeneous film of barium ferrite is f by the pyrolytic decomposition of citrate precursor. Hence, the films are annealed at 70^{o}C for 3h in air to obtain crystallized single phase ferrite thin.

2.3 Structural analysis

Morphological and microstructural studies of materials are necessary to understand the different properties. Cation distribution information is vital to interpret the results of the experimental studies. For characterization of the materials, the experimental studies with X-ray diffraction is adopted. Hence theoretical aspects of different techniques are described.

2.3.1 X-ray diffraction

X-ray crystallography is an fundamental approach to figure out the molecular and atomic structure of a crystal, in which a crystal is radiated by the beam of X-rays which will diffract into different directions. One can find out the three dimensional image of electron density by mapping the intensity and the angle of diffraction of the diffracted. This outcome will help to assess the positions of the atoms in the crystal, type of chemical bond presents in the crystal, crystal defects and other numerous information.

The necessary condition for the constructive interference between the scattered radiations is given by Bragg's condition. According to Bragg, the constructive interference between radiations from successive planes will happen when their path difference is become equal to the integral multiple of wavelengths i.e. [149]

$$2d_{hkl} \sin\theta = n\lambda \qquad (2.1)$$

Where, d_{hkl} is corresponds to inter planer spacing, θ is the angle of incidence, λ is the X-ray wavelength and n is the order of the diffraction. The schematic illustration of Bragg's diffraction technique is depicted in Fig. 2.3.

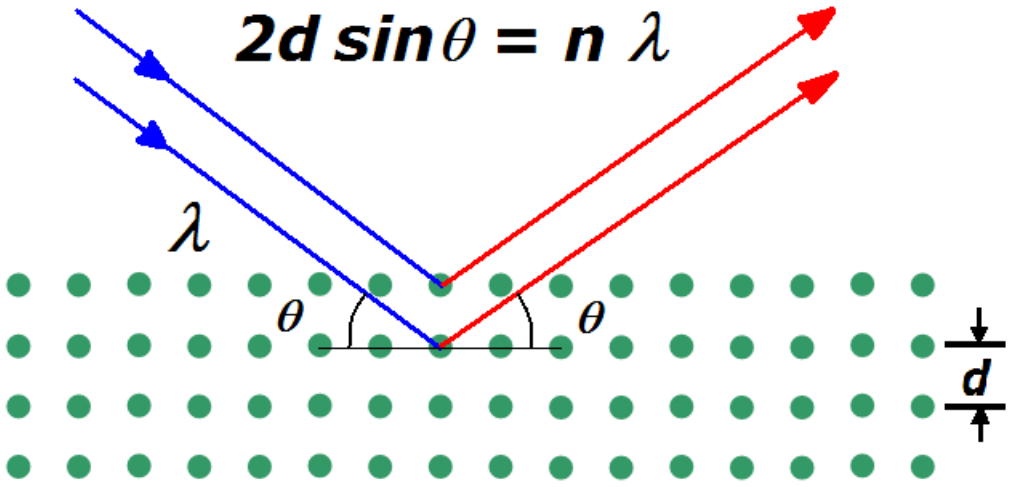

Fig. 2.3. Illustration of Bragg's diffraction technique.

These X-ray spectra provides us information about grain size, lattice parameter and crystal structure of the samples. In order to study micro-structural properties. X-ray diffraction patterns have been obtained for all the prepared ferrites. It is also used for the detection of various phases present in the samples. All the prepared samples can be indexed as the single-phase cubic spinel structure.

2.3.1.1 Indexing and crystal structure

The diffraction spectra shows the intensity variation with 2θ. The pattern exhibits some peaks which are corresponds to the maximum intensity due to diffraction. The indexing of the sample, i.e., the (h k l) values of different planes can be found out by the

software named powder X-ray software created by Chen Dong [150]. The crystal structure of the sample can be verified from the JCPDS database of ICDD (International Centre for Diffraction Data).

2.3.1.2 Lattice parameter

The lattice constant of the sample can be figured from the Bragg's diffraction condition as illustrated in equation (2.1). Hence for the first order diffraction

$$d_{hkl} = \frac{\lambda}{2\sin\theta} \qquad (2.2)$$

For cubic crystal structure

$$d_{hkl} = \frac{a}{(h^2+k^2+l^2)^{1/2}} \qquad (2.3)$$

Where, *a* is the unit cell parameter or lattice constant.

Hence the lattice constant can be expressed as

$$a = \frac{\lambda}{2}\sqrt{\left[\frac{h^2+k^2+l^2}{sin^2\theta}\right]} \qquad (2.4)$$

2.3.1.3 Crystalline size

Not just the peak position in a θ-2θ measurement contains significant data on the sample under study also the width or full width at half maximum (FWHM) of the diffraction peak give some data too. For a perfect crystal, the width of the interference peak is proportional to the inverse thickness of the crystalline layer.

The crystalline size or grain size of the crystal can be assessed by using the Debye-Scherrer's equation as

$$D = \frac{0.9\lambda}{\beta cos\theta} \qquad (2.5)$$

Where, β is the FWHM (full width at half maxima)

2.3.1.4 X-ray density

The X-ray density can be estimated by using the equation:

$$D_X = \frac{8M}{N_A a^3} \qquad (2.6)$$

Where, N_A represent the Avogadro's number, a is lattice parameter and M implies the molecular weight.

2.3.1.5 Bulk density

The bulk density (D_B) of the specimen is obtained by using the following formula

$$D_B = \frac{\text{Mass of the sample (M)}}{\text{Volume of the sample (V)}} \qquad (2.7)$$

2.3.1.6 Porosity

The percentage of porosity of the samples can be assessed by the expression:

$$P = \left(\frac{D_X - D_B}{D_X}\right) \times 100\% \qquad (2.8)$$

2.4 Dielectric properties

Dielectric constant is an important feature of ferrite and dielectric materials. Permittivity and permeability are two important parameters to decide the dielectric and magnetic behavior of a material. Ferrite materials are very often good dielectrics. For most applications of ferrite materials, the dielectric constant (ε′), dielectric loss (ε″) and dielectric loss tangent (tanδ) are the vital practical parameters, and the investigation of the dielectric behaviors supply some essential data about the acceptability of the material for numerous applications. It also determines the medium parameters like velocity of electromagnetic wave propagation, reflectance, characteristic impedance etc. These important parameters have been used in designing of resonator for circulators and impedance matching of microwave components using ferrite and dielectric materials. The selection of the operating frequency is determined by the size of resonator and impedance matching ensures the minimum reflection when medium changes. These parameters play a vital role in designing low loss transmission cables, transformer designing and other medical applications.

2.4.1 Dielectric constant

For a particular sample, the proportion of the capacitance of a capacitor with the specimen as dielectric material to the capacitance of that capacitor without dielectric material is termed as the dielectric constant of that specimen. It measures the amount of electrical charge at an applied electric field in which the material can defy. The capacitance, C_0 for a parallel plate capacitor in free space can be written as

$$C_0 = \frac{\varepsilon_0 A}{d} \qquad (2.9)$$

Where ε_0 is the free space permittivity, 'A' is the area of electrode and 'd' is the separation between two electrodes.

When a dielectric material is introduced in the space between two plates of a parallel plate capacitor, then the capacitance will increased by a factor ε_r, which is termed as the dielectric constant of the specimen. In this way, for a parallel plate capacitor with a dielectric substance between two plates, the capacitance C may expressed as

$$C = \frac{\varepsilon_r \varepsilon_0 A}{d} \qquad (2.10)$$

Hence, the dielectric constant of a ferrite may be estimated by the equation as

$$\varepsilon_r = C/C_0 \qquad (2.11)$$

The dielectric constant is a complex quantity and can be written as

$$\varepsilon * = \varepsilon' + i\varepsilon'' \qquad (2.12)$$

Where ε' represents real or dispersive part of the dielectric constant and ε'' represents imaginary part or the dissipative part of the dielectric constant, which measures the dielectric losses. The real part (ε') of dielectric constant measures the amount electrical energy form an applied electric field can be hold in a material. The imaginary part (ε'') is known as the loss factor. It measures the amount of energy dissipated in the material when it is exposed to an applied electric field. The dielectric loss factor involves both the effects of dielectric loss and resistivity.

The dielectric constant (ε) of a ferrite is influenced by its microstructure. It also depends on the insulating grain and grain boundaries which are formed during the synthesis process. Ferrite material has a very high dielectric constant (~10^5) at low frequency region. However, it decreases with frequency to a low value (~ 10) at the frequency of microwave region. This high value of dielectric constant (ε) of ferrite materials was clearly interpreted by Maxwell [151] and Wagner [152] with the help of their interfacial polarization model considering that the ferrite has inhomogeneous dielectric structure. The origin of interfacial polarization model can be elucidated from the resistivity distribution of the ferrite material. The resistivity distribution is induced by the irregular arrangement of oxygen ions created at the time of sintering process [153]. Oxygen ions have two loosely bound electrons and when the ions are exposed to a small applied electric field, then the electron – ion distributions are distorted and therefore, the polarization is induced.

Additionally, in accordance with interfacial polarization model by Maxwell and Wagner, Koops [154] suggested a phenomenological theory to explain the dielectric dispersion of the ferrite. As per this model, the ferrite comprises of conducting grains isolated by insulating grain boundaries. The hopping conduction is mainly caused by Fe^{2+} ions at the time of sintering. During the cooling process, the presence of oxygen ions inside the pores again oxidizes Fe^{2+} ions present in the outer layers of grains into Fe^{3+} ions. Hence, the conducting grains surrounding the non-conducting grain boundaries are created. This mechanism of polarization could not explain the frequency variation of dielectric constant of ferrite. Koops suggested that the dielectric dispersion in ferrites can be replaced by an

equivalent electrical circuit comprising of resistances and capacitances in series and parallel combination.

2.4.2 Dielectric loss tangent

In an ideal dielectric material the charging current and the voltage are in opposite phase. Be that as it may, in real dielectrics along with the charging current associated with the stored electric charge by the dipoles, a loss current should also be took account for. The loss current appears due to the long-range migration of charges like; dc conduction. Hence the electrical energy will dissipated due to the oscillating nature of dipoles. As the dielectric isn't loss free, it is basically described by a complex dielectric constant. The net current is a complex quantity in the actual dielectric materials which drives the voltage with an angle (90-δ), where δ is known as the loss angle. The dielectric loss factor (ε") can be estimated in term of tangent loss factor (tanδ) describe by the equation

$$tan\delta = \frac{\varepsilon''}{\varepsilon'} \qquad (2.13)$$

The tangent of dielectric loss angle can also be determined by utilizing the equation

$$tan\delta = \frac{1}{2\pi f R_S C_S} \qquad (2.14)$$

where δ is the loss angle, f is the frequency of the applied field, R_S represents equivalent series resistance and C_S is called the equivalent series capacitance.

2.5 Complex impedance spectroscopy

Complex impedance spectroscopy is a renowned and dynamic method which has been efficiently utilized to investigate different electrical behaviors such as conductivity, dielectric properties and relaxation process of the electro-ceramic materials. These analyses help us to understand different processes in electro-ceramic materials, like, bulk effects or the grain boundary contribution in the frequency and temperature space.

The complex impedance of a polycrystalline ferrite sample can be expressed as [155]

$$Z^* = Z' + jZ'' = \frac{1}{j\omega C_0 \varepsilon^*} \tag{2.15}$$

Again,

$$\frac{1}{Z^*} = \frac{1}{Z'+jZ''} = \frac{1}{R} + j\omega C \tag{2.16}$$

Where,

$$Z' = \frac{\frac{1}{R}}{\left(\frac{1}{R^2}\right)+\omega^2 C^2} \tag{2.17}$$

$$Z'' = \frac{-\omega C}{\left(\frac{1}{R^2}\right)+\omega^2 C^2} \tag{2.18}$$

Where, R and C are the resistance and capacitance of corresponding equivalent circuit. The grain and grain boundary conduction of the material can be represent as the series and parallel combination of resistor and capacitor. The reliance of imaginary

component of complex impedance (Z″) with real component (Z′) is known as Nyquist plot or Cole-Cole plot. Hence the complex impedance can also be illustrated as

$$Z^* = Z' + iZ'' \qquad (2.19)$$

where $$Z' = \frac{R_g}{1+(\omega R_g C_g)^2} + \frac{R_{gb}}{1+(\omega R_{gb} C_{gb})^2} \qquad (2.20)$$

and $$Z'' = \frac{\omega R_g^2 C_g}{1+(\omega R_g C_g)^2} + \frac{\omega R_{gb}^2 C_{gb}}{1+(\omega R_{gb} C_{gb})^2} \qquad (2.21)$$

The activation energy of the ferrite sample may be calculated by utilizing the Arrhenius's equation

$$\tau = \tau_0 \exp\left(\frac{-E_a}{k_B T}\right) \qquad (2.22)$$

Where, τ denotes the relaxation time, k_B is the Plank's constant, T denotes the absolute temperature and E_a denotes the activation energy of the sample.

2.6 Electric modulus

The complex modulus formalism initially has been presented by P. B. Macedo et al. [156] to explore and examine the space charge relaxation phenomena, carrier hopping rate etc. The fundamental preferred standpoint of this portrayal is that the small capacitance value is more imperious and the impact of electrode polarization is stifled here. The electric modulus may be assessed by utilizing the relation written as [157].

$$M^* = \frac{1}{\varepsilon^*} = i\omega C_0 Z^* \qquad (2.23)$$

$$M^* = M' + iM'' = i\omega C_0 (Z' + iZ'') \qquad (2.24)$$

The spectrum of complex electric modulus mainly illustrates the ordering of ionic energies or the configurations in the structure. It also represents some microscopic properties and electrical relaxation of ionic glasses [156, 158]. The main advantage of modulus formalism is that it cut off the effect of polarization at the electrolyte interface. Therefore, the dynamic properties of the material has been focused by the complex electric modulus M (ω) spectrum.

In real dielectric solid, there is a broad and asymmetric modulus spectrum due to the existence of non-Debye type relaxation process. The variation of relaxation time is continuous and is represented by normalized function for the distribution of relaxation times g(t) [159].

In the present case, the electric modulus behavior can be communicated by the altered Kohlrausch-Williums-Watts (KWW) function proposed by Bergman [160]. The imaginary part of the electric modulus ($M"$) is communicated as [161]

$$M" = \frac{M"_{max}}{(1-\beta)+\frac{\beta}{1+\beta}\left[\beta\left(\frac{fmax}{f}\right)+\left(\frac{fmax}{f}\right)^{\beta}\right]} \qquad (2.25)$$

where β is the stretched exponent parameter and f_{max} is the frequency at $M"_{max}$. The estimation of β lies in the range of $0 < \beta \leq 1$. In that case because of the non-Debye type relaxation process the value of β is under 1.

2.7 Electrical conductivity

The conductivity spectroscopy is a vital tool to describe different electrical and electrochemical behavior of ionic conductors [162-164]. Generally, the conductivity can be measured by applying the dc voltage difference across the sample. This results in induce of polarization at electrolyte interface, which is in the opposite direction to the applied field. As a result, the polarization will neutralize the dc voltage and the ionic current will falls with time. To solve the problem, the four-probe method or two reversible electrode techniques are used to estimate the dc conductivity of the samples [163]. Later, the single frequency measurements has been taken, but these techniques are insufficient to understand the complete electrical properties of the samples because the electrochemical processes represented by various individual elements (R, C & L) are frequency dependent [165, 166]. Therefore, the ac method has been evolved to account the impedance of the sample over a frequency range to calculate the both ac and dc conductivity. The bulk conductivity as well as the effects of grain boundary, ionic transport, formation of double layer at the electrode etc. can be found out from the impedance data. Therefore, in current years, the Impedance Spectroscopy (IS) has become an important powerful technique for describing the electrical behaviors of the ionic solids. Also, Impedance Spectroscopy (IS) facilitate the dynamic properties to explain the microscopic nature of the eletro-ceramic [163, 165, 167].

The ac conductivity of a ferrite sample might be assessed from the equation [116] as below

$$\sigma_{ac} = \varepsilon_0 \varepsilon' \omega tan\delta \qquad (2.26)$$

Where, tanδ is the dielectric loss tangent, can be written as

$$tan\delta = \frac{\varepsilon''}{\varepsilon'} \tag{2.27}$$

Hence,

$$\sigma_{ac} = \varepsilon_0 \varepsilon'' \omega \tag{2.28}$$

Where ε_0 is the permittivity at free space, ε' and ε'' are the real and imaginary part of dielectric constant, respectively, and ω is the angular frequency of the external ac field.

The dispersion of ac conductivity of different ferrite samples are generally follows the Jonscher's single power law [113], such as

$$\sigma_{ac} = \sigma_{dc} + A(T)\omega^n \tag{2.29}$$

Where, σ_{dc} is the frequency independent dc conductivity, A(T) is a pre-factor which is temperature dependent and have a unit of conductivity and n is the unit less frequency exponent which is also temperature dependent. The first term associated with the drift mobility of free charge carriers, which dominate at lower frequency. The expression for the dc conductivity suggested by Arrhenius as

$$\sigma_{dc} = \sigma_0 exp\left(\frac{-E_a}{k_B T}\right) \tag{2.30}$$

Where, σ_0 is the temperature independent dc conductivity, k_B is the Plank's constant, T is the absolute temperature and E_a is the activation energy of the material. The second term in equation (2.29) associated with the dielectric relaxation of bound charge, which prevails at high frequency [107].

The variation *n* with temperature reveals then conduction mechanism in spinel ferrites. Different theories have been suggested by variuous research group to find the correlation between ac conductivity and conduction mechanism in ferrite materials. If *n* increases with temperature attains a maxima and then diminishes then this will corresponds to the overlapping large polaron tunneling (OLPT) model of ac conduction. In respect of this model,

$$n = 1 - \frac{8\alpha R_w + 6\beta W_{HO} r_p / R_w}{\left(2\alpha R_w + \beta W_{HO} r_p / R_w\right)^2} \qquad (2.31)$$

And the ac conductivity is

$$\sigma_{ac}(\omega) = \frac{\pi^4 e^2 (k_B T)^2 [N(E_F)]^2 \omega R_w^4}{12\left(2\alpha k_B T + W_{HO} r_p / R_w^2\right)} \qquad (2.32)$$

Where, β is $1/k_B T$, k_B is the Boltzmann's constant, T is the absolute temperature, $N(E_F)$ represents the density of states at Fermi level, r_p is the polaron radius, W_{HO} is the barrier height, α measures the spatial extent of polaron and R_w is the width of tunnel.

If the value of *n* increases with temperature then the conduction mechanism is associated with small polaron tunneling model. According to this model

$$n = 1 - \frac{4}{\ln\left(1/\omega\tau_0\right) - W_H k_B T} \qquad (2.33)$$

And

$$\sigma_{ac}(\omega) = \frac{\pi^4 e^2 k_B T [N(E_F)]^2 \omega R_w^4}{24\alpha} \qquad (2.34)$$

Where, e is the electronic charge, k_B is the Boltzmann's constant, T measures the absolute temperature, α represents the spatial extent of polaron, W_H is the barrier height, R_w is the width of the tunnel and $N(E_F)$ is the density of states at Fermi level.

Again, if n decreases monotonically with temperature then this corresponds to correlated barrier hopping (CBH) conduction mechanism utilizing the following equations, such as

$$n = 1 - \frac{6k_BT}{W_H + k_BT\ln(\omega\tau_0)} \qquad (2.35)$$

And

$$\sigma_{ac}(\omega) = \frac{\pi^3}{24}[N(E_F)]^2\varepsilon\varepsilon_0\omega R_W^6 \qquad (2.36)$$

Where, ε is the dielectric permittivity of the medium and ε_0 is the free space permittivity [128].

2.8 Magnetic properties

The magnetic properties of different magnetic materials are however so important to find out the magnetic nature and ordering of the materials. Some extensive magnetic properties for technological applications can retrieve from the following studies.

2.8.1 Saturation magnetization (M_S)

The study of Ms reveals the nature of exchange interactions of octahedral and tetrahedral sub-lattices in ferrite. The saturation magnetization $4\pi M_S$ of a magnetic

material can be defined as the net dipole moment per unit volume at 0K, when dipole moments corresponds to all the molecules are aligned in the direction of external applied field. Hence,

$$M_S = N \sum \mu_i \qquad (2.37)$$

Where, N is the number of dipoles present in unit volume and μ_S is the dipole moment of each molecule.

Saturation magnetization is an inherent and intrinsic property of the ferrite material. It mainly depends upon the chemical composition and electronic structure of the constituents. Domain structure in ferrimagnetic materials is analogous to that of ferromagnetic materials. Net magnetic moment in ferrites arises because of orbital motion of electrons and uncompensated electron spins associated with cations oriented in parallel direction. Ionic magnetic moment is also accountable because of the spin motion of the electrons. A very small amount of moment is also expected for the orbital motion of electron due to the quenching of orbital motion by the crystalline field [168].

It is necessary to consider the contribution from the substituent cations and all the anions present in the ferrite structure to the magnetic moment. The oxygen ions on acquisition of two electrons into partially filled 2p subshell do not contribute to magnetic moment. In case of Fe^{2+} ions there exist six electrons in d shell resulting in four uncompensated spins in the 3d subshell. Assuming no contribution to magnetic moment from orbital quenching motion, the Fe^{2+} ions will have a magnetic moment of $4\mu_B$.

Fe^{3+} ion has five electron spins in 3d shell and hence, the magnetic moment associated with it, is $5\mu_B$.

Strong quantum mechanical forces of interaction acted between the electronic spin of the neighboring ions. According to Neel [24] there exists three types of exchange interactions namely AA, BB and AB interactions. The nature of these interactions was similar to that in antiferromagnetic materials [24]. The resultant magnetization of the lattice is the contrast between magnetization of B and A sub-lattices, i.e,

$$M = M_B - M_A \tag{2.38}$$

Later the Neel‟s theory was modified by Yafet and Kittel [152] taking into account antiferromagnetic A-A and B-B interactions, which were earlier considered small compared to A-B reactions. It was proposed that triangular arrangement of magnetic moments in each sub-lattice and the resultant moment distributions is called a canted spin arrangement. One possible explanation is magnetic dilution of one sub lattice due to the existence of non-magnetic ions. This model explains the deviation of experimental value of 4πMs from the theoretical value based on Neel's model.

The saturation magnetization is the very important properties of ferrites which give the information of cation distribution and indirectly give the strengths of various exchange interactions.

2.8.2 Curie temperature (T_C)

Magnetic properties in a material originate from the uncompensated electron spins of the magnetic ions. The exchange interaction tends to orient these spins [169] which gives the non-zero magnetic moment. A perfect arrangement of dipoles in sub lattice takes place at absolute zero temperature and the arrangement of spins becomes disordered with temperature. As the temperature increases from 0K the magnetic moments starts randomizing. At the Curie temperature, the randomization becomes complete and the magnetic material becomes paramagnetic. The Curie point is the temperature at which the no aligning effect of exchange interactions. This thermal energy of disordering of random orientation of spins, i.e.

$$E_j = E_{thermal} \tag{2.39}$$

It is obvious that Curie temperature relies upon exchange energy and number of nearest neighbor ions magnetic neighbors. Curie temperature increases as the number of spins per atom increases causing stronger interaction between the neighboring magnetic ions. Curie temperature facilitates the estimation of the temperature up to which the device could be operated effectively.

2.8.3 Initial permeability

Initial permeability is one of the essential property of a magnetic material. It describes the impact of external magnetic field on the status of magnetization of the material. The dielectric constant and initial permeability represents the effect of the electric and magnetic behavior of a medium on the propagation of electromagnetic waves. The

magnetic materials undergo hysteresis, the initial permeability is characterized as the ratio of magnetic flux density B at an infinitesimally small external magnetic field H to that of nonmagnetized sample such as:

$$\mu_i = \frac{1}{\mu_0} \lim_{H \to 0} \frac{B}{H} \qquad (2.40)$$

Where, μ_0 is the permeability in vacuum, B is magnetic flux density and H is the external magnetic field.

In case of alternating applied magnetic field, the magnetization produced in the material and the applied field are not in same phase due to dissipation of energy as a result of damping. Hence, the initial permeability is a complex quantity and related as:

$$\mu_i = \mu'_i + i\mu''_i \qquad (2.41)$$

Where, μ'_i represents the dispersive element and μ''_i is the dissipative element of initial permeability. Both of these μ'_i and μ''_i varies with frequency and hence μ_i is frequency dependent.

In order to justify the aspects of ferromagnetism, Weiss had [170] predicted the presence of ferromagnetic domains in the light of molecular field theory. In such domain, all the spins are lined up parallel to one another. The layer, which segregates these adjacent domains, is known as Block wall or "domain wall" [168]. In these "domain wall", the direction of magnetization continuously changes from one direction to another. The various possible mechanisms, responsible for initial permeability, are attributed to the simultaneous rotation of the spins in each Weiss domain and to the reversible displacement

or bulging of domain walls [168, 171]. The former is known as domain rotation and the latter is known as domain wall motion. The theory of initial permeability was explained by Globus model [172]. This model successfully explains the various reversible and irreversible processes of magnetization. Initial permeability also depends on the method of synthesis of the ferrite samples. Larger grain size has higher value of initial permeability [173]. In additional to this, it also depends on the grain size distribution and porosity [174, 175].

2.8.4 Magnetic hysteresis

When a ferromagnetic substance is placed into an external magnetic field, it gets magnetized due to domain wall displacement and domain wall rotation. These two processes can take place irreversibly when a non- magnetized sample is going through magnetization and demagnetization process, which gives rise to Hysteresis loop. In the magnetization curve the values of magnetic induction (B) fall out of phase with applied field at higher values of applied magnetic field (H) approaches and finally reach saturation value (B_s). When the magnetic field is gradually decreases to zero the remaining magnetic induction (B) is termed as remanent induction B_r. The reversed applied magnetic field is required to decrease the induction B to zero is known as coercive field or coercivity H_c. The area enclosed in the hysteresis loop is the amount of magnetic energy losses acquired in the magnetization procedure. The hysteresis losses and coercivity can likewise be related with the irreversible domain dynamics. If the domain walls can easily displaced then the coercive force will be quite small. The coercive field H_c of a magnetic material becomes high if there is some restriction on domain wall motion results in high Hysteresis

losses. The domain wall rotation is mainly due to the intrinsic microstructural properties of the material. The domain wall displacement also relies upon the microstructural properties of the materials. Hence the shape of the loop depends on chemical composition, porosity, sizes and shape of the pores and grain size of the material. In ferrites a high value of induction is required for industrial applications even for low applied field therefore the study of hysterics ferrites (B-H Curve studies) became very important.

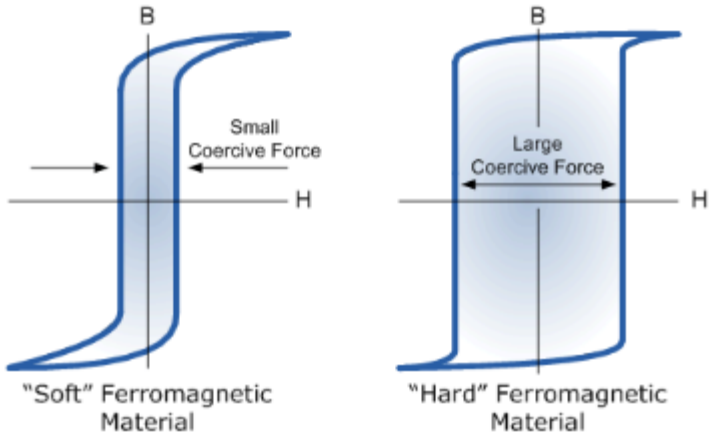

Fig. 2.4. Hysteresis loop of different shape (a) Rectangular B-H loop. (b) Square B-H loop.

Hysteresis loop of a magnetic material is observed due to its magnetization at different levels with different mechanisms relating to microstructure of the material. Formation of the loop and the nature of the loop shape depends on some conditions. Loop shape may be either rectangular or square type (Fig. 2.4). Ferrites, that have applications at micro wave frequency range, in general exhibit rectangular Hysteresis loop (RHL). Since these ferrites with different chemical composition exhibit RHL, there should be some common conditions to display RHL such as grain size, stoichiometric defects, chemical

composition and distribution of ions in the octahedral site(s). Liorzou et al. [176] gave an analytical expression for Hysteresis loop size. This model correlates the magnetization, both as a function of magnetic field and domain wall position in the grain. The minimum required field (H) to move domain wall from its starting point to final state can be done by minimizing the sum of three energies. These are domain wall frictions at the grain boundary, the domain wall surface and the magneto static energy acting on the wall as a magnetic pressure. Hence, formation of the magnetization curve takes place.